



Ortho-II band folding in $\text{YBa}_2\text{Cu}_3\text{O}_{7-\delta}$ films revealed by angle-resolved photoemission

Y. Sassa,^{1,*} M. Radović,^{2,3} M. Månsson,^{1,2,4} E. Razzoli,^{2,3} X. Y. Cui,^{3,†} S. Pailhès,⁵ S. Guerrero,⁶ M. Shi,³ P. R. Willmott,³ F. Miletto Granozio,⁷ J. Mesot,^{1,2} M. R. Norman,⁸ and L. Patthey^{3,‡}

¹Laboratory for Neutron Scattering, ETH Zürich and Paul Scherrer Institut, CH-5232 Villigen PSI, Switzerland

²Laboratory for Synchrotron and Neutron Spectroscopy, EPFL, CH-1015 Lausanne, Switzerland

³Swiss Light Source, Paul Scherrer Institut, CH-5232 Villigen PSI, Switzerland

⁴Laboratory for Solid State Physics, ETH Zürich, CH-8093 Zürich, Switzerland

⁵Laboratoire PMCN, UMR 5586, Université Lyon 1, CNRS-Université de Lyon, F-Villeurbanne 69622, France

⁶Condensed Matter Theory Group, Paul Scherrer Institut, CH-5232 Villigen PSI, Switzerland

⁷CNR-SPIN, Complesso Universitario Monte S. Angelo, I-80126 Napoli, Italy

⁸Materials Science Division, Argonne National Laboratory, Argonne, Illinois 60439, USA

(Received 28 January 2011; revised manuscript received 9 March 2011; published 22 April 2011)

We present an angle-resolved photoelectron spectroscopy study of $\text{YBa}_2\text{Cu}_3\text{O}_{7-\delta}$ films *in situ* grown by pulsed laser deposition. We have successfully produced underdoped surfaces with ordered oxygen vacancies within the CuO chains resulting in a clear ortho-II band folding of the Fermi surface. This indicates that order within the CuO chains affects the electronic properties of the CuO_2 planes. Our results highlight the importance of having not only the correct surface carrier concentration, but also a very well ordered and clean surface in order that photoemission data on this compound be representative of the bulk.

DOI: [10.1103/PhysRevB.83.140511](https://doi.org/10.1103/PhysRevB.83.140511)

PACS number(s): 74.25.Jb, 74.72.-h, 74.78.-w, 71.18.+y

Since the discovery of high-temperature superconductors (HTSCs), the $\text{YBa}_2\text{Cu}_3\text{O}_{7-\delta}$ (Y123) compound has been the subject of many experimental and theoretical studies.¹⁻⁴ Recently, interest in this material was renewed when quantum oscillation experiments in high magnetic fields in underdoped ortho-II ordered $\text{YBa}_2\text{Cu}_3\text{O}_{6.5}$ ($\text{YBCO}_{6.5}$) revealed that the Fermi surface (FS) reconstructs into one² or several⁵ pockets. Indeed, theoretical predictions have shown that ortho-II ordered $\text{YBCO}_{6.5}$ should display band folding, giving rise to pockets.^{3,4} Further, for other cuprate HTSCs, evidence for such pockets has been reported by angle-resolved photoelectron spectroscopy (ARPES).^{6,7} However, for ordered $\text{YBCO}_{6.5}$, no pockets or band folding have been directly observed by ARPES.¹

The crystal structure of Y123 [Fig. 1(a)] differs slightly from other HTSCs. In addition to the CuO_2 planes, it also contains one-dimensional (1D) CuO chains along the b axis that donate charge carriers (holes) to the superconducting planes. It is also well established that Y123 displays a wide variety of superstructures⁸ caused by oxygen-vacancy order within the chains. One in particular is the ortho-II phase, characterized by ordered oxygen vacancies within every second CuO chain [Fig. 1(b)]. This alternation of filled and empty chains along the b axis induces a unit-cell doubling along the a axis, i.e., a reduction of the Brillouin zone, and hence band folding is expected.^{3,4} Unfortunately, ARPES experiments on Y123 and especially the ortho-II phase are notoriously difficult. One reason is that the crystal structure lacks a natural cleavage plane, and hence cleaved, the surface contains both CuO and BaO terminations, giving different contributions to the total ARPES intensity.⁹ Moreover, due to polarity, the cleaved surface tends to be strongly overdoped^{1,9} even though the bulk is underdoped. As a result, details of the electronic properties have remained elusive. To avoid the problem with self-hole doping of Y123, Hossain *et al.*¹ performed an *in situ* evaporation of potassium (K) onto the cleaved surface. Although the correct hole doping was

achieved, the importance of oxygen-vacancy ordering as well as surface termination remained unresolved and the expected ortho-II band folding^{3,4} was not detected. Due to the absence of experimental evidence, the ortho-II potential was assumed to be too weak, and such band folding was not considered in many theoretical models.¹⁰

In this Rapid Communication we present a high-resolution ARPES study of heteroepitaxial Y123 films, grown *in situ* by pulsed laser deposition (PLD).¹¹ The ARPES experiments were performed on the Surface/Interface Spectroscopy (SIS) X09LA beamline at the Swiss Light Source, Paul Scherrer Institut, Villigen, Switzerland. The beamline was set to circular polarized light with a photon energy, $h\nu = 70$ eV, and data were acquired using both Gammadata Scienta SES-2002 and VG-Scienta R4000 electron analyzers. The energy resolution was set to 15–25 meV and the momentum resolution parallel and/or perpendicular to the analyzer slit was chosen as $\sim 0.009/0.019$ \AA^{-1} . Data were acquired in the temperature range $T = 9$ –120 K using the six degree-of-freedom CARVING manipulator. The binding-energy scale was calibrated with a copper reference sample in direct electrical and thermal contact with the film. The base pressure of the UHV system was below 5×10^{-11} mbar during the entire measurement and no sign of sample and/or data quality degradation was observed. Our results were reproduced on several occasions, using more than ten different samples grown under the same conditions.

The 100-nm-thick Y123 films were grown on TiO_2 (B -side) terminated SrTiO_3 (STO) substrates, resulting in a CuO chain termination of the Y123 surface.¹² Reflection high-energy electron-diffraction (RHEED) measurements of the films show a streaky pattern [Fig. 1(d)], suggesting a clear two-dimensional (2D) growth with an atomically flat crystalline surface. Moreover, additional peaks around, e.g., $(0 \ 1/2)$ and $(0 \ -1/2)$ [Fig. 1(e)] can be distinguished, suggesting a unit-cell doubling. Also the low-energy electron diffraction (LEED) pattern [Fig. 1(c)] displays a clear (2×1) reconstruction, as

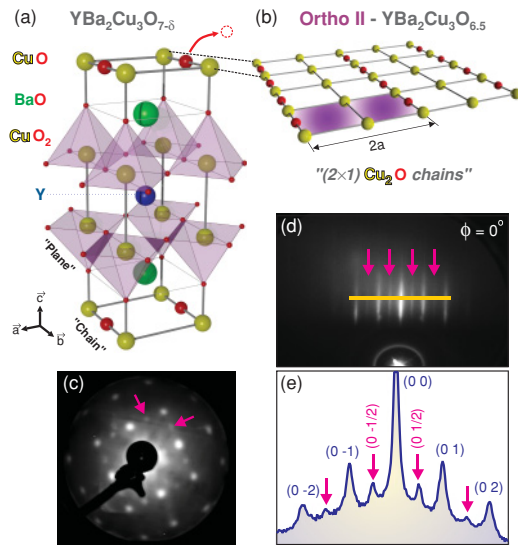


FIG. 1. (Color online) (a) Structure of Y123 showing the CuO_2 planes and CuO chains. (b) Half-filled and ordered (2×1) ortho-II chains corresponding to $n = 6.5$. (c) Low-energy electron diffraction (LEED) pattern shows extra spots from the (2×1) chain order (arrows) in both directions because of twinning. (d) Reflection high-energy electron diffraction (RHEED) pattern. (e) Cut along the solid line in (d). Superstructure peaks at, e.g., $(0 -1/2)$ and $(0 1/2)$ (arrows) indicate the unit-cell doubling.

indicated by the extra weaker spots. It is also clear that the film is twinned since the (2×1) spots appear in both directions. The bulk properties of the film were verified *ex situ* by x-ray diffraction (XRD) measurements. The XRD pattern shows a very good c -axis orientation and a narrow (FWHM $\approx 0.08^\circ$) rocking curve of the YBCO (005) reflection (not shown).

By a direct *in situ* transfer between the PLD and ARPES UHV chambers, we have been able to measure the Y123 films *as grown* (without cleaving). In Fig. 2(a) a typical ARPES spectrum is shown, which was acquired at cut ① [Fig. 2(d)] and $T = 10$ K. Two strong dispersive features are clearly observable, but also four supplementary weaker bands are visible that were not present in previous ARPES measurements on Y123.¹ From the dispersion it is clear that the supplementary bands are created by a folding of the main bands. This is consistent with the extra lines and/or points in the RHEED and/or LEED patterns (Fig. 1) that reveal a unit-cell doubling. The folded bands are even more visible in Fig. 2(b), where the result of a Lorentzian fit of the momentum distribution curve (MDC) at the Fermi level (E_F) is shown. Figure 2(c) represents the energy distribution curve (EDC) at the Fermi wave vector (k_F) for one of the main bands in Fig. 2(a) (blue dashed vertical line). A sharp quasiparticle (QP) peak is visible slightly below E_F , indicating the presence of a superconducting gap.

By acquiring ARPES spectra for multiple momentum cuts, we have mapped out the FS of the Y123 film. Figure 2(d) shows the spectral intensity map integrated ± 5 meV around E_F and Fig. 2(e) shows the underlying FS integrated ± 5 meV around a binding energy $E_B = 35$ meV (i.e., below the gap). Centered around (π, π) , we find a weaker pocketlike feature (square) associated with the folded bands and unit-cell

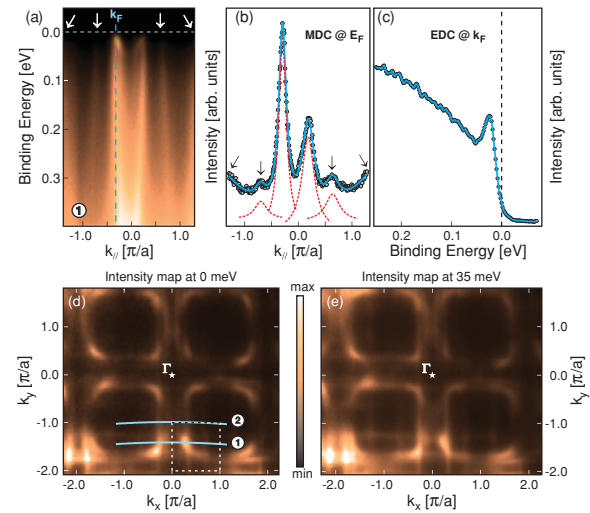


FIG. 2. (Color online) (a) ARPES spectrum acquired at cut ① in k space as indicated by the solid line in (d). (b) Momentum distribution curve (MDC) at the Fermi level (E_F) and a Lorentzian fit (solid and dashed lines). (c) Energy distribution curve (EDC) at k_F and $T = 10$ K. (d) Spectral intensity map obtained by energy integration of ARPES spectra ± 5 meV about E_F . The two solid white lines mark two specific cuts ① and ② in k space. (e) Same as (d) but ± 5 meV about $E_B = 35$ meV. From photon-energy-dependent measurements, a photon energy of $h\nu = 70$ eV was chosen in order to maximize the spectral intensity from the CuO_2 planes while suppressing the contribution from the CuO chains.

doubling, as mentioned above. By extracting the surface-hole doping (p_{surf}) from the FS area, $p_{\text{surf}} = 0.1 \pm 0.02$ is obtained, corresponding to an oxygen content $n = 7 - \delta \approx 6.5$, i.e., $\text{YBCO}_{6.5}$. It can be concluded that the surface of the film has both the correct hole doping and the necessary (vacancy) order to be a good representation of ortho-II $\text{YBCO}_{6.5}$.

Figure 3(a) represents the EDC at k_F [blue dashed line showed in Fig. 2(a)] as a function of temperature. At low temperature ($10 \text{ K} \leq T \leq 60 \text{ K}$), a clear QP peak is observed. At higher T , this peak decreases significantly and almost vanishes at $T = 70$ K. The appearance of such a coherent peak below T_c is a good indication of the presence of a superconducting state. In order to estimate the superconducting gap value, the EDCs are symmetrized with respect to E_F [Fig. 3(b)]. The extracted gap size for cuts ① at $T = 10$ K is $\Delta_1 = 22 \pm 3$ meV. Increasing T reduces the gap value until it closes at $T = 70$ K, indicating that $T_c \approx 65$ K. From the value of T_c it is deduced that $p^{T_c} \approx 0.106$,¹³ which is in good agreement with the value extracted from the FS area. Figure 3(c) shows the EDC at k_F at the antinode for cut ② [Fig. 2(d)] at $T = 10$ – 120 K. Contrary to cut ①, the QP peak at $T = 10$ K is strongly suppressed, which is a common feature of underdoped cuprates. As in Fig. 3(b), the EDCs are symmetrized and the obtained gap size is $\Delta_2 = 52 \pm 4$ meV. The values of Δ_1 and Δ_2 are consistent with a strongly anisotropic gap having its maximum at the antinodal point. Above the superconducting transition at $T = 120$ K, the symmetrized EDCs show that Δ_2 remains open, while Δ_1 has closed at $T = 70$ K. This strongly suggests the existence of a pseudogap state, again confirming that the surface of the film is indeed underdoped.

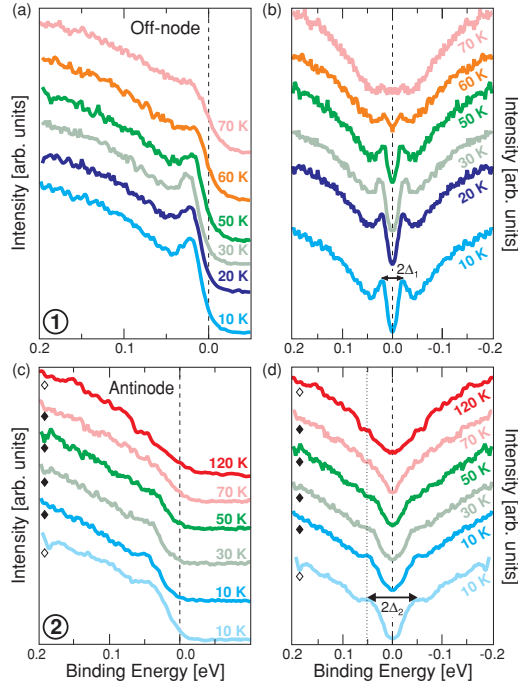


FIG. 3. (Color online) (a) Energy distribution curves (EDCs) for cut ① in Fig. 2(d) as a function of temperature, $T = 10\text{--}70$ K. (b) Symmetrization of the EDCs in (a) showing the opening of the superconducting gap ($\Delta_1 = 22 \pm 3$ meV) below $T_c \approx 65$ K. (c) EDCs for cut ② in Fig. 2(d) for $T = 10\text{--}120$ K. \diamond and \blacklozenge are the results from two different samples. (d) Symmetrization of the EDCs in (c) showing the presence of a superconducting gap below T_c and a pseudogap above T_c ($\Delta_2 = 52 \pm 4$ meV).

To consider the effect of the ortho-II order on the electronic structure as only a simple band folding along the a axis is a highly simplified picture. For instance, it has been shown by nuclear magnetic resonance (NMR) that the vacancy order causes a charge imbalance between the Cu atoms sitting below filled and/or empty chains.¹⁴ Naturally, a coupling between the bands of the chains and the superconducting CuO_2 planes is expected. Bascones *et al.* theoretically demonstrated that for ortho-II, due to interlayer coherence and oxygen ordering, the bonding (B) and anti-bonding (AB) bands of Y123 are each split into two bands, α and a quasi-1D β due to zone folding.¹⁵ Taking into account the $2a$ periodicity of the ortho-II phase, the resulting dispersion of the CuO_2 plane can be expressed according to¹⁵

$$\varepsilon_{\alpha,\beta}^{\text{AB,B}}(\mathbf{k}) = -2t \cos k_y - 2t''(\cos 2k_x + \cos 2k_y) - \mu \pm t_{\perp}(\mathbf{k}) \pm \left[4 \cos^2 k_x (t - 2t' \cos k_y)^2 + \frac{V^2}{4} \right]^{\frac{1}{2}}, \quad (1)$$

where μ is the chemical potential, t is the nearest-neighbor hopping integral, t' and t'' the second- and third-nearest-neighbor intraplane hopping integrals, t_{\perp} is the interlayer hopping integral (bilayer splitting), and V is the ortho-II potential. The first and second \pm signs set the AB-B bands and the α - β bands, respectively. Here, V is set constant since from local-density approximation (LDA) calculations, the ortho-II potential is only slightly k dependent near the nodes.¹⁵ Further,

since the existence of bilayer splitting in the underdoped regime remains unclear and cannot be distinguished in our data, t_{\perp} is neglected. This is consistent with very recent ARPES data recorded for different dopings of Y123 surfaces, which demonstrated that the bilayer splitting is progressively reduced upon underdoping and vanishes below $p \approx 0.15$.¹⁶ The FS can be adequately fitted by the tight-binding model described by Eq. (1), giving $t = 558 \pm 50$ meV, $t'/t = 0.49 \pm 0.03$, $t''/t' = 0.5 \pm 0.03$, $\mu = -469 \pm 90$ meV, and $V = 75$ meV. Figure 4(a) shows the calculated FS of the ortho-II sample considering the tight-binding parameters mentioned above. It is clear that the reduction of the Brillouin zone induces a drastic change in the shape but also the number of FS sheets. For a twinned sample, the FS will be folded along both the $(\pi/2, 0)$ - $(\pi/2, \pi)$ as well as the $(0, \pi/2)$ - $(\pi, \pi/2)$ lines. Figure 4(b) shows the calculated FS for a twinned ortho-II sample and Fig. 4(c) shows the corresponding simulated intensity map at 0 meV with an energy broadening of 25 meV. In the latter, the upper-right-hand quadrant represents the experimental data [dashed square area in Fig. 2(d)] and the filled circles are extracted from Lorentzian fits of the MDCs at E_F for different k momenta. Figure 4(d) shows the filled circles (symmetrized in momentum) along with the calculated twinned FS. By comparing the calculated intensity map with the data [Fig. 4(c)] and by overlaying the model onto the experimental points [Fig. 4(d)], it is clear that there is very good agreement.

In summary, we have been able to measure Y123 films by ARPES, a task previously thought not possible due to oxygen deficiency causing an insulating surface.¹⁷ By

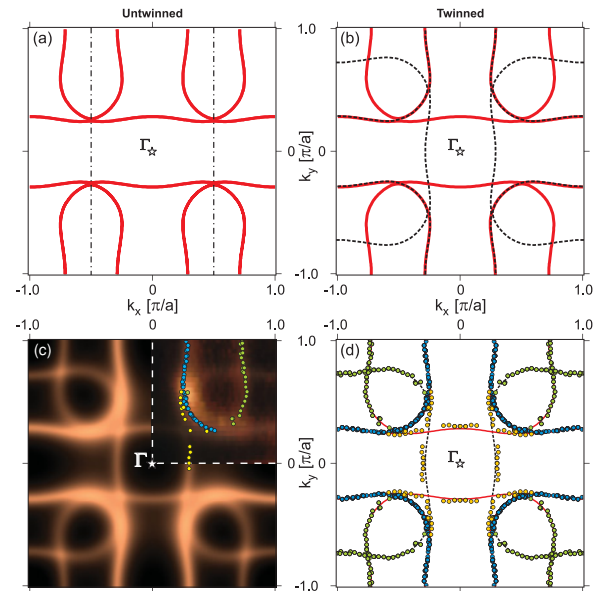


FIG. 4. (Color online) (a) Tight-binding Fermi surface (FS) for ortho-II $\text{YBCO}_{6.5}$ calculated using Eq. (1). (b) Same as (a) but after the addition of a second, 90° rotated, domain caused by twinning (dashed lines). (c) Simulated spectral intensity map at E_F . The upper-right-hand quadrant shows the experimental data [extracted from the dashed square in Fig. 2(d)] and the filled circles represent k_F as determined from Lorentzian fits of the MDCs at E_F . (d) Overlay of experimentally determined k_F (filled circles) and calculated ortho-II FS from (b).

growing oxygen-ordered Y123 films *in situ*, a clear surface representation of ortho-II band folding is made evident by ARPES. Our results thereby confirm theoretical^{3,4} and experimental expectations.¹⁸ We connect this to a (2×1) surface reconstruction caused by ordered oxygen vacancies that help to stabilize the Y123 surface. Our experiments clearly highlight the importance of having not only the correct carrier concentration, but also a very well ordered and clean surface to facilitate ARPES data representative of the compound's true nature. This could also explain why the ortho-II band folding was not found by Hossain *et al.*¹ Even though they evidently managed to obtain the correct (under)doping of the surface by K evaporation, the essential ordering of oxygen vacancies was not fulfilled. For other compounds it has been shown that charge-carrier concentration *and* ion-vacancy ordering are of equal importance for the magnetic¹⁹ as well as electronic properties.²⁰ In this case, we have successfully shown how oxygen vacancy ordering in the CuO chains of the surface influences the electronic properties of the superconducting CuO₂ planes in Y123 films. In fact, such unidirectional

band folding could contribute to the strong breaking of the fourfold rotational symmetry of the CuO₂ planes observed by the Nernst effect.²¹ This work clears the way to directly investigate such matters by performing ARPES measurements on, preferably, untwinned Y123 samples. We would also like to emphasize that having obtained a more accurate view of the *bulk* electronic structure in underdoped Y123, the ortho-II folding can no longer be ignored.^{1,10} Instead, our results give solid experimental support for theoretical models that consider a combination of ortho-II band folding and magnetic^{22,23} or *d*-density wave (DDW) order,²⁴ which could be important for explaining the quantum oscillation results.^{2,5}

We are grateful to Andrea Damascelli for valuable discussions, as well as Christian M. Schlepütz for his support. This research was supported by the Swiss National Science Foundation, MaNEP, and the Foundation BLANCEFLOR Boncompagni-Ludovisi née Bildt. M.N. was supported by the US DOE, Office of Science, under Contract No. DE-AC02-06CH11357.

*yasmine.sassa@psi.ch

[†]Present address: University Duisburg-Essen, Physics Department, D-47048 Duisburg, Germany.

[‡]luc.patthey@psi.ch

¹M. A. Hossain, J. D. F. Mottershead, D. Fournier, A. Bostwick, J. L. McChesney, E. Rotenberg, R. Liang, W. N. Hardy, G. A. Sawatzky, I. S. Elfimov, D. A. Bonn, and A. Damascelli, *Nat. Phys.* **4**, 527 (2008).

²N. Doiron-Leyraud, C. Proust, D. LeBoeuf, J. Levallois, J.-B. Bonnemaison, R. Liang, D. A. Bonn, W. N. Hardy, and L. Taillefer, *Nature (London)* **447**, 565 (2007).

³A. Carrington and E. A. Yelland, *Phys. Rev. B* **76**, 140508(R) (2007).

⁴I. S. Elfimov, G. A. Sawatzky, and A. Damascelli, *Phys. Rev. B* **77**, 060504(R) (2008).

⁵A. Audouard, C. Jaudet, D. Vignolles, R. Liang, D. A. Bonn, W. N. Hardy, L. Taillefer, and C. Proust, *Phys. Rev. Lett.* **103**, 157003 (2009).

⁶J. Chang, Y. Sassa, S. Guerrero, M. Månsson, M. Shi, S. Pailhès, A. Bendounan, R. Mottl, T. Claesson, O. Tjernberg, L. Patthey, M. Ido, M. Oda, N. Momono, C. Mudry, J. Mesot, and *New J. Phys.* **10**, 103016 (2008).

⁷E. Razzoli, Y. Sassa, G. Drachuck, M. Månsson, A. Keren, M. Shay, M. H. Berntsen, O. Tjernberg, M. Radovic, J. Chang, S. Pailhès, N. Momono, M. Oda, M. Ido, O. J. Lipscombe, S. M. Hayden, L. Patthey, J. Mesot, and M. Shi, *New J. Phys.* **12**, 125003 (2010).

⁸Q. Wang, H. Rushan, D. L. Yin, and Z. Z. Gan, *Phys. Rev. B* **45**, 10834 (1992).

⁹V. B. Zabolotnyy, S. V. Borisenko, A. A. Kordyuk, J. Geck, D. S. Inosov, A. Koitzsch, J. Fink, M. Knupfer, B. Büchner, S.-L. Drechsler, H. Berger, A. Erb, M. Lambacher, L. Patthey, V. Hinkov, and B. Keimer, *Phys. Rev. B* **76**, 064519 (2007).

¹⁰N. Harrison, *Phys. Rev. Lett.* **102**, 206405 (2009).

¹¹P. R. Willmott and J. R. Huber, *Rev. Mod. Phys.* **72**, 315 (2000).

¹²J. M. Huijbregtse, J. H. Rector, and B. Dam, *Physica C* **351**, 183 (2001).

¹³R. Liang, D. A. Bonn, and W. N. Hardy, *Phys. Rev. B* **73**, 180505 (2006).

¹⁴Z. Yamani, W. A. MacFarlane, B. W. Statt, D. Bonn, R. Liang, and W. N. Hardy, *Physica C* **405**, 227 (2004).

¹⁵E. Bascones, T. M. Rice, A. O. Shorikov, A. V. Lukoyanov, and V. I. Anisimov, *Phys. Rev. B* **71**, 012505 (2005).

¹⁶D. Fournier, G. Levy, Y. Pennec, J. L. McChesney, A. Bostwick, E. Rotenberg, R. Liang, W. N. Hardy, D. A. Bonn, I. S. Elfimov, and A. Damascelli, *Nat. Phys.* **6**, 905 (2010).

¹⁷M. Abrecht, D. Ariosa, D. Cloetta, D. Vobornik, G. Margaritondo, and D. Pavuna, *J. Phys. Chem. Solids* **65**, 1391 (2004).

¹⁸D. L. Feng, A. Rusydi, P. Abbamonte, L. Venema, I. Elfimov, R. Liang, D. A. Bonn, W. N. Hardy, C. Schuster-Langeheine, S. Hulbert, C.-C. Kao, and G. A. Sawatzky, e-print [arXiv:cond-mat/0402488](https://arxiv.org/abs/cond-mat/0402488).

¹⁹T. F. Schulze, P. S. Hafliger, C. Niedermayer, K. Mattenberger, S. Bubenhofer, and B. Batlogg, *Phys. Rev. Lett.* **100**, 026407 (2008).

²⁰L. Balicas, Y. J. Jo, G. J. Shu, F. C. Chou, and P. A. Lee, *Phys. Rev. Lett.* **100**, 126405 (2008).

²¹R. Daou, J. Chang, David LeBoeuf, Olivier Cyr-Choinière, Francis Laliberté, Nicolas Doiron-Leyraud, B. J. Ramshaw, Ruixing Liang, D. A. Bonn, W. N. Hardy, and Louis Taillefer, *Nature (London)* **463**, 28 (2010).

²²H. Oh, Hyoun Joon Choi, Steven G. Louie, Marvin L. Cohen, e-print [arXiv:0912.2450v1](https://arxiv.org/abs/0912.2450v1).

²³J.-M. Carter, D. Podolsky, and H.-Y. Kee, *Phys. Rev. B* **81**, 064519 (2010).

²⁴D. Podolsky and H.-Y. Kee, *Phys. Rev. B* **78**, 224516 (2008).